A R C H I V E S O F M E T A L L U R G Y A N D M A T E R I A L S
Volume 53 2008 Issue 3

M. LUBAS*, J. ZBROSZCZYK** M. NABIAŁEK**, J. OLSZEWSKI**, K. SOBCZYK**, W. CIURZYŃSKA**, M. SZOTA*, P. BRĄGIEL***, J. P. JASIŃSKI****, J. ŚWIERCZEK**

MECHANICAL AND MAGNETIC PROPERTIES OF BULK AMORPHOUS $Fe_{59}Co_{15}Zr_2Y_4Me_5B_{15}$ (Me=Mo OR Nb) ALLOYS

MECHANICZNE I MAGNETYCZNE WŁAŚCIWOŚCI MASYWNYCH STOPÓW AMORFICZNYCH $Fe_{59}Co_{15}Zr_2Y_4Me_5B_{15}$ (Me=Mo LUB Nb)

Some structural, magnetic and mechanical properties of bulk $Fe_{59}Co_{15}Zr_2Y_4Me_5B_{15}$ (Me=Mo or Nb) alloys in the form of plates 0.5 mm thick obtained by a suction casting method are presented. X-ray diffraction and Mössbauer spectroscopy show that the bulk $Fe_{59}Co_{15}Zr_2Y_4Me_5B_{15}$ alloy is fully amorphous, whereas $Fe_{59}Co_{15}Zr_2Y_4Me_5B_{15}$ alloy is partially crystallized. The grains of α-FeCo crystalline phase with the volume fraction of 0.03 are embedded in the inhomogeneous amorphous matrix. The Vickers hardness of the fully amorphous $Fe_{59}Co_{15}Zr_2Y_4Me_5B_{15}$ alloy is the same on the surface (HV_{surf}) and in cross section (HV_{cross}) of the sample and its average value equals to 10.4 GPa. For the partially crystallized plates of $Fe_{59}Co_{15}Zr_2Y_4Me_5B_{15}$ alloy the surface hardness ($HV_{surf=9.6}$ GPa) is lower than in cross section ($HV_{cross=10.3}$ GPa) of the sample. The alloys containing Nb exhibits higher wear resistance than the alloy with Mo. Both alloys are soft ferromagnets.

Keywords: Mössbauer spectroscopy, coercivity, DSC curves, hardness, wear resistance

W pracy są prezentowane badania struktury, właściwości magnetycznych i mechanicznych masywnych stopów $Fe_{59}Co_{15}Zr_2Y_4Me_5B_{15}$ (Me=Mo lub Nb) w postaci płytek o grubości 0,5 mm, produkowanych metodą zasysania. Badania z wykorzystaniem dyfrakcji promieni X i spektrometrii mössbauerowskiej pokazują, że masywny stop $Fe_{59}Co_{15}Zr_2Y_4Me_5B_{15}$ jest w pełni amorficzny, natomiast stop $Fe_{59}Co_{15}Zr_2Y_4Me_5B_{15}$ jest częściowo skrystalizowany. Ziarna fazy krystalicznej αFeCo są otoczone niejednorodną matrycą amorficzną i zajmują 3% objętości próbki.

Twardość stopu amorficznego $Fe_{59}Co_{15}Zr_2Y_4Me_5B_{15}$ jest taka sama na powierzchni próbki, jak i w przekroju poprzecznym. Średnia wartość twardości dla tego stopu HV=10,4 GPa. Twardość częściowo skrystalizowanej płytki stopu $Fe_{59}Co_{15}Zr_2Y_4Me_5B_{15}$ na jej powierzchni jest mniejsza ($HV_{surf=9,60}$ GPa) niż w przekroju poprzecznym ($HV_{cross=10,30}$ GPa). Stop $Fe_{59}Co_{15}Zr_2Y_4Me_5B_{15}$ wykazuje większą odporność na ścieranie niż stop $Fe_{59}Co_{15}Zr_2Y_4Me_5B_{15}$. Obydwa badane stopy są ferromagnetykami magnetycznie miękkimi.

1. Introduction

It is commonly known that the bulk amorphous alloys are multicomponent systems. In order to obtain an amorphous structure in bulk materials three rules must be fulfilled: 1) the alloy should consist of more than three elements, 2) atomic radii of main components should differ more than 12 %, 3) main components should exhibit the negative heat of mixing [1]. The bulk amorphous alloys with different shapes are prepared at lower quenching rates than classical amorphous ribbons. The structure of these alloys is at least partially relaxed and shows higher density of atoms than classical amorphous materials [2]. The multicomponent system limits atomic diffusion which in turns suppresses nucleation and growth of crystalline grains. The possibility of mixing of many different elements enables us to obtain wide range of materials with unusually physical properties. One of the important group of the bulk amorphous materials are transition metal – based alloys exhibiting excellent soft magnetic properties and simultaneously good mechanical features. The refractory transition elements i.e. Mo, Nb, W, Y and Hf do not possess the magnetic moment but have larger atomic radii than magnetic Fe, Co and

* INSTITUTE OF ENGINEERING MATERIALS, CZĘSTOCHOWA UNIVERSITY OF TRCHNOLOGY, ARMII KRAJOWEJ AV. 19, 42-200 CZĘSTOCHOWA, POLAND
** INSTITUTE OF PHYSICS, CZĘSTOCHOWA UNIVERSITY OF TECHNOLOGY, ARMII KRAJOWEJ AV. 19, 42-200 CZĘSTOCHOWA
*** INSTITUTE OF PHYSICS, J. DŁUGOSZ UNIVERSITY, ARMII KRAJOWEJ AV. 13/15, 42-200 CZĘSTOCHOWA, POLAND
**** ASSOCIATION OF POLISH INVENTORS AND RATIONALIZERS, UL. RYDYGIERA 8, 01-793 WARSAW, POLAND

Ni atoms and influence the magnetic properties of the amorphous alloys [3]. The addition even small amount of late transition elements (about 1 at %) to the amorphous alloys involves also changes of their mechanical properties, i.e. Young modulus, hardness and wear resistance [4].

The purpose of this paper is to study the structure, thermal stability, some mechanical and magnetic properties of the bulk amorphous $Fe_{59}Co_{15}Zr_2Y_4Me_5B_{15}$ (Me=Mo or Nb) alloys.

2. Experimental procedure

The bulk amorphous $Fe_{59}Co_{15}Zr_2Y_4Me_5B_{15}$ (Me=Mo or Nb) alloys were prepared by a suction casting method [5] in an inert argon atmosphere. The samples were in the form of plates 0.5 mm thick.

The amorphicity of the as-cast samples was verified by X-ray diffraction and Mössbauer spectroscopy. The X-ray diffraction patterns were recorded by a conventional X-ray diffractometer at room temperature for both as-received and powdered samples.

Mössbauer spectra were recorded for powdered samples. The Mössbauer spectra were analyzed accordingly to the Hesse – Rübartsch method [6] and the distributions of hyperfine field parameters were derived.

The differential scanning calorimetry (DSC) curves were recorded at the heating rate of 10 K/min. The mechanical properties i.e. hardness, abrasive wear resistance and density were studied for the as-received plates. These investigations were carried out at room temperature. The hardness was tested on the surface and in cross section of the sample. Additionally, hardness was measured for the corresponding crystalline ingots. A Vickers hardness tester FUTURETECH 740 working under the load of 200 G was used. The abrasive wear resistance measurements were conducted by a KULOTESTER [7] on the sample surface. The wear resistance was determined from the micrographs taken by an optical microscope. The density was measured by the Archimedes method. The samples were weighed in the air and toluene.

Coercivity and magnetic saturation polarization of the samples were determined from hysteresis loops and magnetization curves, respectively. These measurements were performed using a vibrating sample magnetometer. The samples for those studies were in the form of discs 4 mm in diameter and 0.5 mm thick. The demagnetization effect was taken into account.

3. Results and discussion

X-ray diffraction (XRD) patterns of the bulk $Fe_{59}Co_{15}Zr_2Y_4Me_5B_{15}$ (Me=Mo or Nb) alloys after solidification are presented in Fig. 1. The XRD pattern of the $Fe_{59}Co_{15}Zr_2Y_4Me_5B_{15}$ alloy (Fig. 1 a) displays only a broad maximum at about $2\theta = 50°$, implying a fully amorphous state. However, the XRD pattern of the $Fe_{59}Co_{15}Zr_2Y_4Me_5B_{15}$ plate (Fig. 1b) exhibits an additional, pronounced peak at $2\theta = 60°$ corresponding to the crystalline α-FeCo. It indicates that this alloy is partially crystallized.

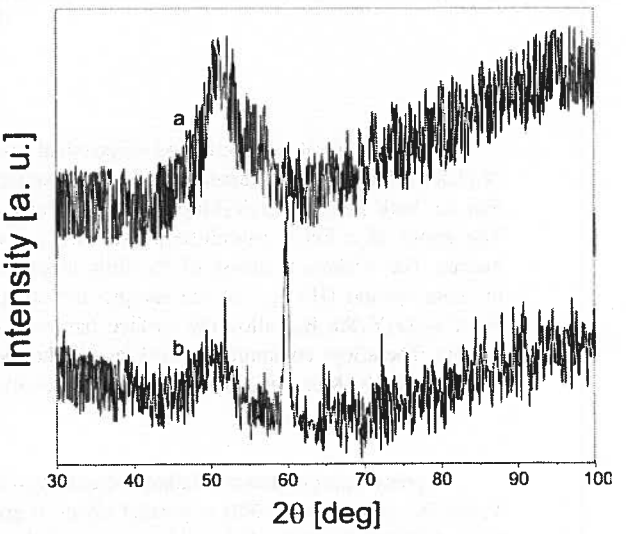

Fig. 1. X-ray diffraction patters for the as-received fully amorphous $Fe_{59}Co_{15}Zr_2Y_4Me_5B_{15}$ (a) and partially crystallized $Fe_{59}Co_{15}Zr_2Y_4Me_5B_{15}$ (b) alloys

Fig. 2 a shows the transmission Mössbauer spectrum and corresponding hyperfine magnetic field distribution of $Fe_{59}Co_{15}Zr_2Y_4Me_5B_{15}$ alloy. It is seen that the spectrum consists of six broad and overlapped lines which is characteristic of Fe-based amorphous alloys. The hyperfine magnetic field distribution is wide (Fig. 2 b) and at least two components may be distinguished suggesting the presence of regions in the sample with different iron concentrations. The Mössbauer spectrum and obtained from it the hyperfine magnetic field distribution for $Fe_{59}Co_{15}Zr_2Y_4Me_5B_{15}$ alloy are depicted in Fig. 2 c, d. The Mössbauer spectrum is well fitted by two Zeeman sextets, corresponding to the amorphous matrix and crystalline α-FeCo phase. In the hyperfine magnetic field distribution corresponding to the amorphous matrix one can see three components which give evidence that this phase is very inhomogenous [8]. The high field component in the hyperfine magnetic field distribution is ascribed to the crystalline α-FeCo phase. The hyperfine field parameters and the crystalline phase composition obtained from the Mössbauer spectra analysis are col-

lected in Table I. It can be seen that the average magnetic hyperfine field induction of $Fe_{59}Co_{15}Zr_2Y_4Me_5B_{15}$ alloy is lower than that for the amorphous phase of $Fe_{59}Co_{15}Zr_2Y_4Me_5B_{15}$ material. The iron concentration in α-FeCo phase with the volume fraction of 0.03 is equal to 84 at % (Table I).

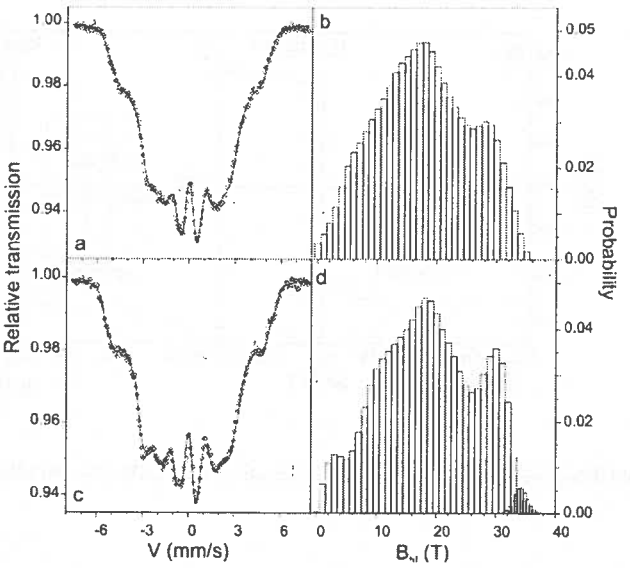

Fig. 2. Transmission Mössbauer spectra (a, c) and corresponding hyperfine magnetic field distributions (b, d) for the as-received $Fe_{59}Co_{15}Zr_2Y_4Me$ (a, b) and $Fe_{59}Co_{15}Zr_2Y_4Me_5B_{15}$ (c, d) alloys

TABLE I

The average values of the hyperfine magnetic field induction (B_{avam}) in the amorphous phase and their standard deviation (ΔB_{am}), effective hyperfine magnetic field induction for the crystalline phase (B_{effcr}), the volume fraction of the crystalline phase (V_{cr}) and the Fe concentration in it for the as-received $Fe_{59}Co_{15}Zr_2Y_4Me_5B_{15}$ and $Fe_{59}Co_{15}Zr_2Y_4Me_5B_{15}$ alloys

alloy composition	B_{avam} [T]	ΔB_{am} [T]	B_{effcr} [T]	V_{cr}	Fe [at. %]
$Fe_{59}Co_{15}Zr_2Y_4Me_5B_{15}$	17.72	7.94	-	-	-
$Fe_{59}Co_{15}Zr_2Y_4Me_5B_{15}$	18.56	7.95	34.21	0.03	84

DSC curves recorded at the heating rate of 10 K/min are shown in Fig. 3. At the temperature of about 600 K small endothermic peaks in DSC curves which seem to be related to the structure changes within the amorphous state are visible. In the case of $Fe_{59}Co_{15}Zr_2Y_4Me_5B_{15}$ alloy the crystallization starts at about 890 K, whereas for $Fe_{59}Co_{15}Zr_2Y_4Me_5B_{15}$ alloy the crystallization process is more complicated and two separated small maxima at 890 K and 930 K are observed. It seems to be caused by the partial crystallization of that alloy during the preparation leading to more inhomogeneous amorphous matrix.

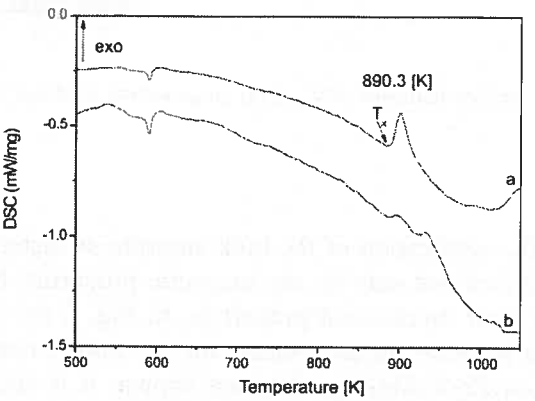

Fig. 3. DSC curves for the as- received $Fe_{59}Co_{15}Zr_2Y_4Me_5B_{15}$ and $Fe_{59}Co_{15}Zr_2Y_4Me_5B_{15}$ alloys obtained at the heating range of 10 K/min

Both investigated alloys are soft ferromagnetic materials and exhibit low coercivity equal to 16 A/m (Fig. 4a) and 25 A/m (Fig. 4b) for $Fe_{59}Co_{15}Zr_2Y_4Me_5B_{15}$ and $Fe_{59}Co_{15}Zr_2Y_4Me_5B_{15}$ alloys, respectively. Moreover, these alloys have relatively high magnetic saturation polarization which amounts to 1.03 T for the former and 1.18 T for the latter alloy.

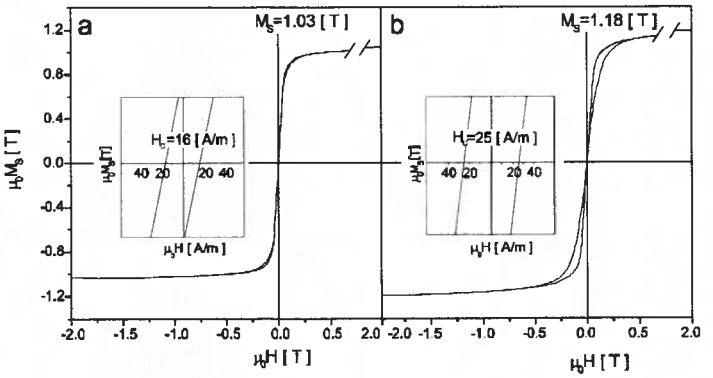

Fig. 4. Hysteresis loops of as-quenched $Fe_{59}Co_{15}Zr_2Y_4Me_5B_{15}$ (a) and $Fe_{59}Co_{15}Zr_2Y_4Me_5B_{15}$ (b) alloys

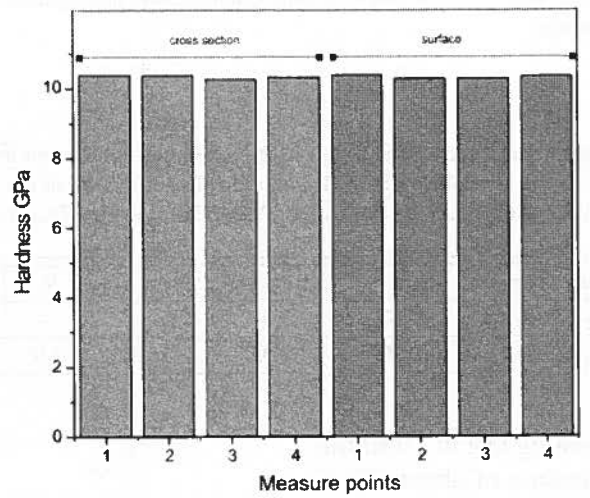

Fig. 5. Surface hardness (HV_{surf}) (a) cross-section hardness (HV_{cross}) (b) of the fully amorphous $Fe_{59}Co_{15}Zr_2Y_4Me_5B_{15}$ alloy

The application of the bulk amorphous materials is determined not only by the magnetic properties but also by their mechanical properties. In Fig. 5 the results of the hardness measurements for the bulk amorphous $Fe_{59}Co_{15}Zr_2Y_4Me_5B_{15}$ alloy are shown. It is seen that the hardness on the sample surface (HV_{surf}) and in cross section (HV_{cross}) is practically the same and does not change from point to point confirming the homogeneity of the alloy. The average value of the hardness amounts to 10.4 GPa. In the case of the partially crystallized bulk $Fe_{59}Co_{15}Zr_2Y_4Me_5B_{15}$ alloy the cross section hardness is higher than the surface hardness and equals to 10.3 GPa and 9.6 GPa, respectively (Fig. 6). The investigated alloys are harder than the crystalline and other non-magnetic bulk amorphous alloys [9, 10]. In Table II the density and the average values of the hardness measured on the surface and in the cross section of the sample are listed for both investigated alloys. The optical micrographs of the sample surface of the bulk amorphous $Fe_{59}Co_{15}Zr_2Y_4Me_5B_{15}$ and partially crystallized $Fe_{59}Co_{15}Zr_2Y_4Me_5B_{15}$ alloys subjected to the wear resistance measurements are presented in Figs. 7 and 8. It is seen that Nb containing alloy exhibits higher wear resistance than Mo containing one. It is worth adding that the bulk amorphous $Fe_{59}Co_{15}Zr_2Y_4Me_5B_{15}$ alloy is brittle.

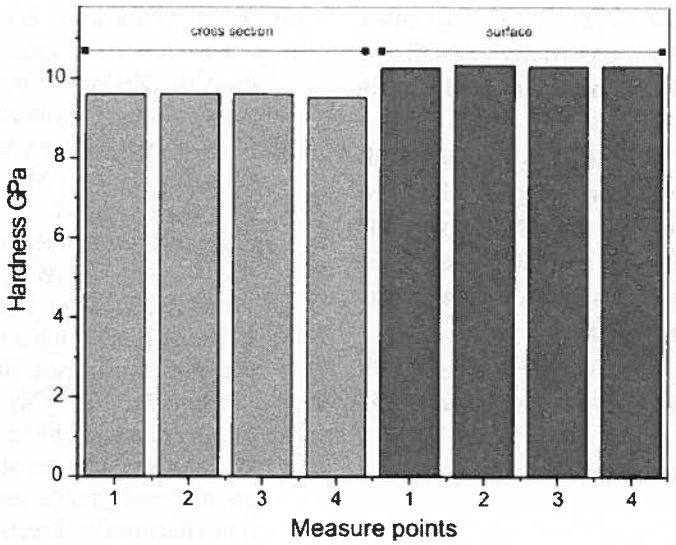

Fig. 6. Surface hardness (HV_{surf}) (a) cross-section hardness (HV_{cross}) (b) of the partially crystallized $Fe_{59}Co_{15}Zr_2Y_4Me_5B_{15}$ alloy

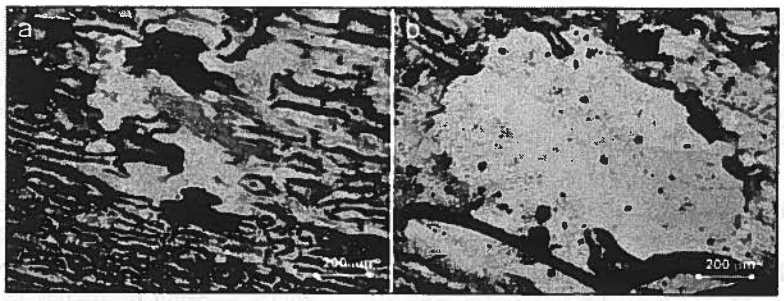

Fig. 7. The optical micrograph of $Fe_{59}Co_{15}Zr_2Y_4Me_5B_{15}$ sample surface subject to 1 h and 3 h abrasive wear resistance test

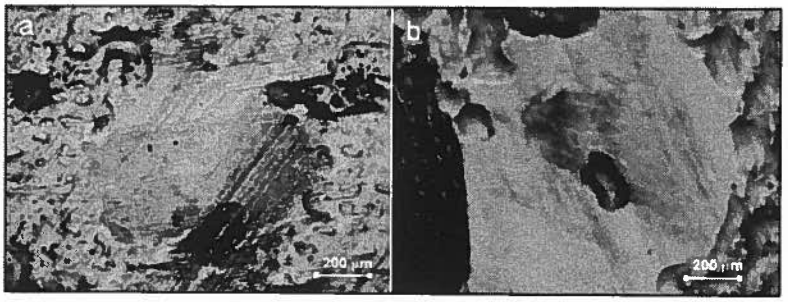

Fig. 8. The optical micrograph of $Fe_{59}Co_{15}Zr_2Y_4Me_5B_{15}$ sample surface subject to 1 h and 3 h abrasive wear resistance test

TABLE 2

Density (ρ), surface (HV_{surf}) and cross section (HV_{cross}) hardness of the fully amorphous bulk $Fe_{59}Co_{15}Zr_2Y_4Me_5B_{15}$ and partially crystallized $Fe_{59}Co_{15}Zr_2Y_4Me_5B_{15}$ alloys

alloy composition	$\rho[10^3 kg/m^3]$	HV_{surf} [GPa]	HV_{cross} [GPa]
$Fe_{59}Co_{15}Zr_2Y_4Me_5B_{15}$	8.4	10.32	10.34
$Fe_{59}Co_{15}Zr_2Y_4Me_5B_{15}$	8.0	10.30	9.57

4. Conclusion

- The bulk $Fe_{59}Co_{15}Zr_2Y_4Me_5B_{15}$ alloy in the form of plates in the as-quenched state is fully amorphous whereas $Fe_{59}Co_{15}Zr_2Y_4Me_5B_{15}$ alloy in the as-received state is partially crystallized and consists of α-FeCo grains embedded in the inhomogeneous amorphous matrix.

- The bulk amorphous $Fe_{59}Co_{15}Zr_2Y_4Me_5B_{15}$ alloy crystallizes in one stage. For the partially crystallized $Fe_{59}Co_{15}Zr_2Y_4Me_5B_{15}$ alloy complex crystallization process is observed.
- The fully amorphous bulk $Fe_{59}Co_{15}Zr_2Y_4Me_5B_{15}$ alloy exhibits larger hardness than the partially crystallized $Fe_{59}Co_{15}Zr_2Y_4Me_5B_{15}$ one. Moreover, the hardness of the former alloy is almost the same on the sample surface and in cross section confirming the homogeneity of this material.
- The fully amorphous bulk $Fe_{59}Co_{15}Zr_2Y_4Me_5B_{15}$ alloy is more wear resistant than $Fe_{59}Co_{15}Zr_2Y_4Me_5B_{15}$ one
- The both investigated alloys are soft magnetic materials.

REFERENCES

[1] A. Inoue, Stabilization of metallic supercooled liquid and bulk amorphous alloys, Acta Mater. **48**, 279 (2000).

[2] J. Olszewski, J. Zbroszczyk, H. Fukunaga, W. H. Ciurzyńska, K. Narita, A. Błachowicz, M. Hasiak, B. Wysłocki, Structure evolution and magnetic properties of annealed $Fe_{77-x-y}Cu_xNb_ySi_{13}B_{10}$, J. Phys. IV France **8**, 131 (1998).

[3] H. Chiriac, N. Lupu, Bulk amorphous (Fe, Co, Ni)$_{70}$(Zr, Nb, M)$_{10}B_{20}$ (M=Ti, Ta or Mo) soft magnetic alloys, J. Magn. Magn. Mater. **215-216**, 394 (2000).

[4] W. M. Wang, A. Gebert, S. Roth, U. Kuehn, L. Schultz, Glass formability and fragility of $Fe_{61}Co_{9-x}Zr_8Mo_5W_xB_{17}$ (x=0 and 2) bulk metallic glassy alloys, Intermetallics 16, 267 (2008).

[5] J. Zbroszczyk, J. Olszewski, W. Ciurzyńska, M. Nabiałek, P. Pawlik, M. Hasiak, A. Łukiewska, K. Perduta, Glass-forming ability and magnetic properties of bulk $Fe_{61}Co_{10}Zr_{2.5}Hf_{2.5}W_{4-y}Me_yB_{20}$ (y=0 or 2, Me=Mo, Nb, Ti) alloys, J. Magn. Magn. Mater. **304**, e724 (2006).

[6] J. Hesse, A. Rübartsch, Model independent evaluation of overlapped Mössbauer spectra, J. Phys E: Sci. Instrum. **7**, 526 (1974).

[7] M. Betiuk, J. Michalski, K. Burzyński, P. Wach, Revaling the structure of thin coatings and layers in metalographic examinations. Kulotester workstation (Institute of Precision Mechanics, Warsaw), SURFEX Conference 12 June 2007, Poznań, Poland.

[8] J. Olszewski, H. Fukunaga, J. Zbroszczyk, W. H. Ciurzyńska, K. Perduta, M. Hasiak, P. Brągiel, M. Piasecki, J. Lelątko, Nanocrystallization and magnetic properties of $Fe_{85.4}Zr_{6.8-x}M_xB_{6.8}Cu_1$ (x=0 or 1; M=Nb, Nd or Mo) alloys, J. Magn. Magn. Mater. **272-276**, 1422 (2004).

[9] T. Fujita, T. Tarui, T. Ochi, Prediction of hardness distribution in forged steel by neutral network model, Nippon Steel Technical Report **96**, 57 (2007).

[10] Y. Zhang, D. Q. Zhao, M. X. Pan, W. H. Wang, Glass forming properties of Zr-based bulk metallic alloys, J. Non-Cryst. Solids **315**, 206 (2003).

Received: 20 June 2008.